Cooperative Coalition Selection for Quality of Service Optimization in Cluster-Based Capillary Networks

Liumeng Song, *Member, IEEE*, Kok Keong Chai, Yue Chen, *Senior Member, IEEE*, Jonathan Loo, *Member, IEEE*, and John Schormans

***Abstract*—Cooperative multiple-input-single-output (CMISO) scheme has been proposed in the literature to prolong the network lifetime in the cluster-based Internet of Things (IoT) systems. CMISO scheme increases the spatial diversity of wireless channels, however, it reduces the transmit power and thus degrades the quality of service (QoS) performance. In this paper, we formulate the problem of cooperative coalition selection for CMISO scheme to minimize the overall packet error rate (PER). Then, we propose to apply the qubit-based quantum-inspired particle swarm optimization (QPSO) to select the optimum cluster head (CH) and cooperative devices coalition. Simulation results proved that the qubit-based QPSO has faster convergence speed and outperforms Ψ-based QPSO, particle swarm optimization (PSO), and quantum genetic algorithm (QGA) in terms of overall PER.**

***Index Terms*—Cluster, cooperative communication, Internet of Things (IoT) systems, quality of service (QoS) provisioning, quantum-inspired particle swarm optimization (QPSO).**

I. Introduction

INTERNET of Things (IoT) systems are viewed to have potential to improve the operational efficiency of many industrial applications. There is an increasing need of huge numbers of reliable devices equipped with short-range radio interfaces, such as Zigbee, low-power Wi-Fi, etc., to provide connectivity to other devices in IoT systems in order to maintain the operational efficiency.

The capillary networks were introduced to improve reliable and energy efficient communications for the IoT systems. Capillary networks are specific local networks consisting of a group of wireless devices to be connected to other communication infrastructure, such as mobile networks [1]. These networks use clustering mechanism to improve energy efficiency [2]. Clustering mechanism organizes the devices into different clusters and selects cluster heads (CHs), which consequently collect data from all cluster members (CMs) and transmit the collected data to the sink node via communication infrastructure networks. However, the CHs consume more energy compared to other devices in the networks as they take more responsibility and dissipate additional energy to transmit aggregated data to the sink node. Cooperative multiple-input-single-output (CMISO) transmission scheme was then proposed to solve the aforementioned problem [3]. CMISO introduces additional cooperative nodes (Coops) to help CH in long-haul (LH) transmission, which is the most energy consuming phase of the communication between the cluster and the sink node. The Coops and CH in the same cluster form a virtual multiple-input-single-output system to transmit the aggregated cluster data to the sink node by the decode-and-forward technique. Nevertheless, although the cooperative communication can potentially improve energy efficiency, it degrades the end-to-end (ETE) quality of service (QoS) due to the cooperation penalty caused by additional transmission of cooperative nodes.

Xiao and Ouyang [4] proposed a game-theoretic power control algorithm to minimize the total power consumption in a cooperative communication network. Chen *et al.* [5] proposed new partial relay selection schemes for cooperative diversity based on amplify-and-forward relaying in Nakagami-m fading channels.The selection of Coops plays an important role in the network performance was proved in [4] and [5]. Coso *et al.* [6] proposed a cluster-based wireless network, which is optimally designed for minimum ETE outage probability given a per link energy constraint. In particular, the authors derived the optimum fraction of time dedicated to the local broadcast channel and to the LH transmission channel, as well as the optimum power allocation over the two channels. However, the power consumption model in [6] does not consider circuit blocks that have great effect on the performance of CMISO communication as proved by [7]. Yuan *et al.* [8] proposed a cross-layer design to jointly improve the energy efficiency, reliability, and ETE QoS provisioning in cluster-based wireless networks. In the proposed design, a nonlinear constrained optimization model is developed to seek the optimal bit error rate (BER) performance for each link to meet the ETE QoS requirements with a minimum energy consumption. However, the number of Coops is predetermined while [9] proved that the optimum number of Coops varies with different LH transmission distance and distribution of nodes. Wu *et al.* [10] designed a cooperative communication scheme to achieve the optimal solution of a random tradeoff between the outage performance and the network lifetime in a cluster-based wireless network. The outage performance is evaluated by a system design parameter and the outage probability threshold. However, [10] assumes that all the CHs are always located in the center of the cluster. In addition, [6], [8], and [10] focus

Manuscript received May 6, 2016; revised August 24, 2016; accepted October 17, 2016.

L. Song, K. K. Chai, Y. Chen, and J. Schormans are with the School of Electronic Engineering and Computer Science, Queen Mary University of London, London E1 4NS, U.K. (e-mail: l.song@qmul.ac.uk; michael.chai@qmul.ac.uk; yue.chen@qmul.ac.uk; j.schormans@qmul.ac.uk).

J. Loo is with the School of Science and Technology, Middlesex University, London NW4 4BT, U.K. (e-mail: J.Loo@mdx.ac.uk).

Digital Object Identifier 10.1109/JSYST.2016.2630662

on the cooperative communication in LH transmission and do not take the DC phase in the intracluster communication into consideration. In addition, in cluster-based capillary networks, packet error may occur in both intracluster and intercluster channels. For successful ETE transmission, every packet needs to be successfully transmitted across all links.

The aforementioned challenges raise the concerns of the optimization of overall QoS provisioning in the cluster-based capillary networks for IoT systems. In our previous work [11], we proposed to use the qubit-based quantum-inspired particle swarm optimization (QPSO) combined with improved Nondominated Sorting Genetic algorithm (NSGA-II) to achieve the tradeoff between energy efficiency and QoS provisioning in cluster-based capillary networks. Compared with [11], we improve the channel model and energy model as [7] in this paper, which is more realistic, complex, and well accepted in the related research area. Additionally, this paper focuses more on the QoS provisioning in capillary networks. In particular, we formulate the QoS provisioning to be the overall packet error rate (PER) of all devices in the whole transmission process, while we studied only the LH QoS provisioning in [11]. The main contributions of this paper are summarized as follows.

1) First, we formulate the QoS provisioning optimization into the optimum cooperative coalition selection problem with the aim of overall PER minimization. In particular, the BER of intracluster communication with AWGN channel and the BER of intercluster communication with Rayleigh channel are formulated separately. Then the PER of different transmission phases are proposed in terms of BER, packet size and number of transmitters, which allows us to derive the overall PER equation.
2) Second, by utilizing the benchmark function, we simulate and compare two different QPSO algorithms: qubit-based QPSO [12] and Ψ-based QPSO [13]. Although both QPSO algorithms apply quantum coding mechanism, the procedures to encode and update the particles in every generation are different. Particularly, Ψ-based QPSO uses quantum delta potential well model to encode particles, whereas qubit-based QPSO uses quantum theory to encode particles. Besides, Ψ-based QPSO adopts mean optimum position and local attractor to update each generation, whereas qubit-based QPSO adopts local optimum position and global optimum position to update each generation. To the best of our knowledge, no recent literature compare the performance of these two QPSO algorithms, although they were proposed independently and both belong to the QPSO evolutionary algorithm. The simulation results prove that both QPSO algorithm outperforms other evolutionary algorithms such as particle swarm optimization (PSO) and quantum genetic algorithm (QGA), but qubit-based QPSO have faster convergence speed and better performance of getting rid of being trapped in local optimum on its way toward the global optimum.
3) Third, by the cooperation benefit with CH, we propose to select the optimum cooperative coalition by qubit-based QPSO. QPSO combines the quantum computing theory and the evolutionary algorithm so it has the characteristics of strong searching capability, rapid convergence, short-computing time, and small-population size [14]. By taking advantage of the fast convergence and low complexity of QPSO, we formulate the possible cooperative coalitions by the quantum-coded particles. In order to select the optimum Coops for the potential CH candidate, all quantum-coded particles are flown through the whole search space by updating the fitness values, i.e., the overall PER, until reaching the predefined maximum generation.

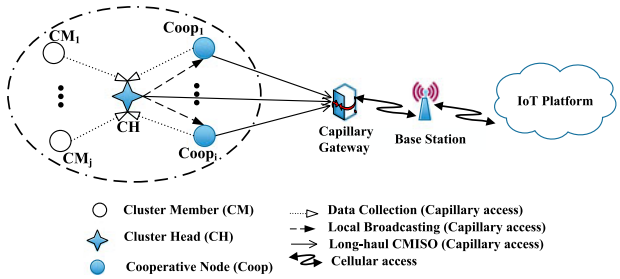

Fig. 1. System model.

This paper is organized as follows. Section II introduces the system model, the energy consumption model, and the problem formulation. In Section III, we explain the qubit-based QPSO in detail and propose the use of qubit-based QPSO algorithm to obtain the optimum CH and Coops cooperative coalition with the objective of minimizing the overall PER. Simulation results are provided in Section IV, and conclusions are drawn in Section V.

II. System Model and Problem Formulation

The system model considers a cluster in a typical energy-limited capillary networks for IoT systems with $\mathcal{N}_{\text{total}}$ devices: one CH, CMs with the number of $\mathcal{N}_{\text{CM}}$ and Coops with the number of $\mathcal{N}_{\text{Coop}}$, as shown in Fig. 1, where $\mathcal{N}_{\text{total}} = 1 + \mathcal{N}_{\text{CM}} + \mathcal{N}_{\text{Coop}}$. In this paper, we assume the additive white Gaussian noise (AWGN) channel with squared power path loss for intracluster communications within the cluster, as well as the frequency-nonselective and slow Rayleigh fading channel for the LH transmission between the cluster and the capillary gateway. In addition, considering the fact that the communication environment is more complex in the LH transmission, we assume the LH transmission with respect to the wavelength gives rise to independent fading coefficients. In developing the strategy, M-ary quadrature amplitude modulation (MQAM) is adopted. The transmission process consists of the following phases.

1) Data collection phase (DC): CH collects and aggregates data from all CMs and Coops.
2) Local broadcasting phase (LB): CH broadcasts the aggregated data to all Coops.
3) LH cooperative transmission phase: CH and Coops jointly encode and transmit the aggregated data to the capillary gateway based on orthogonal space-time block codes (STBC). Then the data information is further forwarded to

the IoT platform through the capillary gateway and base station.

The CMISO transmission consists of the local broadcasting phase, i.e., intracluster communication, and the LH cooperative transmission phase, i.e., intercluster communication. Furthermore, the communication in the DC phase and the local broadcasting phase are performed within the cluster, i.e., intracluster communication.

A. Energy Consumption Model

In this paper, we use the power consumption model as defined in [7]. The total power consumption along a single path can be divided into two main components: power consumption of all power amplifiers P_{PA} and power consumption of all other circuit blocks P_c. As in [7], the power consumption of power amplifiers is linearly dependant on the transmit power P_t. Then the power consumption per link can be expressed as

$$P = P_{PA} + P_c = (1+\alpha)P_t + P_c \tag{1}$$

where $\alpha = \xi/\eta - 1$ with η being the drain efficiency of the RF power amplifier, and ξ being the peak-to-average ratio, which is dependent on the modulation scheme and the associated constellation size [15]. As referred to [7], $\xi = 3(M - 2\sqrt{M}+1)/(M-1)$ in MQAM coded communication.

As discussed in [7], denote the number of transmitter and receiver to be $\mathcal{N}_t$ and $\mathcal{N}_r$, respectively, we estimate the circuit power consumption P_c as

$$\begin{aligned} P_c \approx{}& \mathcal{N}_t(P_{\text{DAC}} + P_{\text{mix}} + P_{\text{filt}}) + 2P_{\text{syn}} \\ &+ \mathcal{N}_r(P_{\text{LNA}} + P_{\text{mix}} + P_{\text{IFA}} + P_{\text{filr}} + P_{\text{ADC}}) \end{aligned} \tag{2}$$

where P_{DAC}, P_{mix}, P_{mix}, P_{filt}, P_{syn}, P_{LNA}, P_{IFA}, P_{filr}, and P_{ADC} are the power consumption values of the D/A converter, the mixer, the active filters at the transmitter side, the frequency synthesizer, the low noise amplifier, the intermediate frequency amplifier, the active filters, and the A/D converter at the receiver side, respectively. P_c consists of the transmitting circuit power P_{ct} and the receiving circuit power P_{cr}.

Then the energy consumption per bit for a general communication link can be formulated as

$$E_{\text{bt}} = \frac{(1+\alpha)P_t + P_c}{R_b} \tag{3}$$

where R_b is the system data rate.

In the MQAM-based connection, the transmit power P_t in (3) can be calculated according to the link budget relationship as follows:

$$P_t = \frac{(4\pi)^2 M_l N_r}{G_t G_r \lambda^2} \cdot \frac{\bar{E}_b}{N_0} R_b d^{\kappa} \tag{4}$$

where d is the distance between transmitter and receiver, κ is the channel path loss exponent, G_t and G_r are the transmitter and receiver antenna gains, respectively, M_l is the link margin that indicates the difference between the receiver sensitivity and the actual received power, N_r is the single-sided power spectral density of the receiver noise, λ is the carrier wavelength, and $\bar{E}_b/N_0$ is the normalized average energy per bit required for a given BER specification to the noise spectral density.

B. Energy Consumption for Intracluster Transmission

In the DC phase, the CH acts as the receiver dissipating the receiving path power consumption, while both CMs and Coops transmit data to the CH, dissipating the transmitting path power consumption. As the assumption of squared power path loss, the energy consumption per bit for this phase E_b^{DC} can be expressed as

$$\begin{aligned} E_b^{\text{DC}} = {}& \sum_{i=1}^{\mathcal{N}_{\text{total}}-1} (1+\alpha)\frac{(4\pi)^2 M_l N_r}{G_t G_r \lambda^2} \cdot \frac{\bar{E}_b}{N_0} d_{i,\text{CH}}^2 \\ &+ \frac{(\mathcal{N}_{\text{total}}-1)P_{\text{ct}} + P_{\text{cr}}}{R_b} \end{aligned} \tag{5}$$

where $d_{i,\text{CH}}$ is the distance between device i and CH.

In the LB phase, CH acts as the transmitter to broadcast the aggregated data to Coops, dissipating the transmitting path power consumption, and all Coops receive data information from the CH, dissipating the receiving path power consumption. Due to the broadcast nature of the wireless channel, if the Coop with the maximum distance denoted by $d_{\max}$ can receive the aggregated data from the CH, the other Coops can simultaneously receive these data. Then the energy consumption per bit for this phase E_b^{LB} can be expressed as

$$E_b^{\text{LB}} = (1+\alpha)\frac{(4\pi)^2 M_l N_r}{G_t G_r \lambda^2} \cdot \frac{\bar{E}_b}{N_0} d_{\max}^2 + \frac{P_{\text{ct}} + \mathcal{N}_{\text{Coop}} P_{\text{cr}}}{R_b}. \tag{6}$$

C. Energy Consumption for LH Transmission

In the LH transmission phase, CH and Coops jointly transmit the aggregated data to the capillary gateway, dissipating the transmitting path power consumption. Thus, the energy consumption per bit for this phase E_b^{LH} is

$$\begin{aligned} E_b^{\text{LH}} = {}& \sum_{i=1}^{\mathcal{N}_{\text{Coop}}+1} (1+\alpha)\frac{(4\pi)^2 M_l N_r}{G_t G_r \lambda^2} \cdot \frac{\bar{E}_b}{N_0} d_{i,g}^{\kappa_{i,g}} \\ &+ \frac{(\mathcal{N}_{\text{Coop}}+1)P_{\text{ct}} + P_{\text{cr}}}{R_b} \end{aligned} \tag{7}$$

where $d_{i,g}$ is the LH distance between the Coops/CH i and the capillary gateway, $\kappa_{i,g}$ is the path loss exponent of the LH transmission and is in the range between 2 and 3.

D. Energy Consumption and Packet Size for Data Aggregation

In [16], the energy dissipation of data aggregation depends on the complexity of data aggregation algorithm, which is denoted by $O(n)$ in this paper. Then the energy dissipation can be formulated as

$$E_{\text{da}} = C_0 + C_1 l \tag{8}$$

where C_0 and C_1 are coefficients depending on the software and CPU parameters, and l is the number of bits required to be aggregated at the CH. Then the energy consumption per bit for data aggregation is determined as

$$E_{\text{bf}} = \frac{C_0 + C_1 l}{l} = \frac{C_0}{l} + C_1. \tag{9}$$

Note that C_0/l can be omitted with a large l. Hence, the energy consumption per bit of algorithm complexity with $O(n)$ is approximately constant. In terms of the experiment results described in [17], E_{bf} is set to be 5 nJ/bit/signal for simulation experiments. Assume all devices transmit packet of the same size, denoted by L, the overall energy consumption for data aggregation is

$$E_{\text{agg}} = \mathcal{N}_{\text{total}} L E_{\text{bf}}. \tag{10}$$

In [18], the amount of data after aggregation is

$$L_{\text{agg}} = \frac{\mathcal{N}_{\text{total}}}{\mathcal{N}_{\text{total}}\gamma - \gamma + 1} L \tag{11}$$

where γ is the aggregation factor.

E. Packet Size of the LH Transmission Phase

In the LH transmission, $\mathcal{N}_{\text{Coop}}$ cooperative nodes together with the CH encode and transmit the transmission sequence based on the aggregated data packet to the capillary gateway using orthogonal STBC. In [19], training overhead is introduced by the CMISO scheme for channel estimation and the number of required training symbols is proportional to the number of transmit antennas. Therefore, the packet size of Coops and CH in the LH transmission is

$$L_c = \frac{F_{\text{block}}}{F_{\text{block}} - \rho_{\text{train}}(N_{\text{Coop}} + 1)} L_{\text{agg}} \tag{12}$$

where F_{block} is the block size of STBC code, $\rho_{\text{train}}(N_{\text{Coop}} + 1)$ is the number of training symbols in each block.

F. Problem Formulation

In [20], the average BER of the intracluster communication with a square constellation (i.e., $b = M/2$ is even and b is called the constellation size of MQAM) and in AWGN channel is given by

$$\bar{P}_{\text{BER}}^{\text{intra}} \doteq \frac{4(1 - 1/\sqrt{M})}{\log_2 M} Q\left(\sqrt{\frac{3\log_2 M}{M-1} \cdot \frac{\bar{E}_b}{N_0}}\right) \tag{13}$$

where $Q(x) = \int_x^\infty \frac{1}{2\pi} e^{-\frac{u^2}{2}} du$.

In [21], the average BER of the intercluster communication with a square constellation MQAM in Rayleigh fading channel is given by

$$\bar{P}_{\text{BER}}^{\text{inter}} \doteq \frac{4}{\log_2 M}\left(1 - \frac{1}{\sqrt{M}}\right)\left(\frac{1-\mu}{2}\right)^{\mathcal{N}_{\text{Coop}}+1} \times \sum_{l=0}^{\mathcal{N}_{\text{Coop}}} \binom{\mathcal{N}_{\text{Coop}} + l}{l}\left(\frac{1+\mu}{2}\right)^l \tag{14}$$

where

$$\mu = \sqrt{\frac{\alpha}{1+\alpha}} \tag{15a}$$

$$\alpha = \frac{1}{\mathcal{N}_{\text{Coop}} + 1} \cdot \frac{3\log_2 M}{2(M-1)} \cdot \frac{\bar{E}_b}{N_0}. \tag{15b}$$

According to [22], the PER is derived as $P_{\text{PER}} = 1 - (1 - P_{\text{BER}})^L$, where L is the packet size in bit. Therefore, the PER of the DC phase, the LB phase and the LH transmission phase, respectively, are given by

$$\bar{P}_{\text{PER}}^{\text{DC}} = 1 - (1 - \bar{P}_{\text{BER}}^{\text{intra}})^{L(N_{\text{total}}-1)} \tag{16a}$$

$$\bar{P}_{\text{PER}}^{\text{LB}} = 1 - (1 - \bar{P}_{\text{BER}}^{\text{intra}})^{L_{\text{agg}} N_{\text{Coop}}} \tag{16b}$$

$$\bar{P}_{\text{PER}}^{\text{LH}} = 1 - (1 - \bar{P}_{\text{BER}}^{\text{inter}})^{L_c(N_{\text{Coop}}+1)}. \tag{16c}$$

Correspondingly, the overall PER in the transmission of all three phases is given by

$$\bar{P}_{\text{PER}}^{\text{overall}} = \bar{P}_{PER}^{\text{DC}} + (1 - \bar{P}_{\text{PER}}^{\text{DC}})\bar{P}_{\text{PER}}^{\text{LB}} + (1 - \bar{P}_{\text{PER}}^{\text{DC}})(1 - \bar{P}_{\text{PER}}^{\text{LB}})\bar{P}_{\text{PER}}^{\text{LH}} \tag{17}$$

where the first term indicates that data error occurs in the transmission of the DC phase, which contributes to the error transmission of the following LB phase and LH transmission phase; the second term means that the data transmission is successful in the DC phase while error occurs in the LB phase; the third term indicates that data transmission of both DC and local transmission phase are successful, however, error occurs in the LH transmission phase.

The research problem is to find the optimum cooperative coalition $\mathcal{C} = \{\text{CH}, \text{Coop}_1, \ldots, \text{Coop}_{\mathcal{N}_{\text{Coop}}}\}$ in order to minimize the overall PER $\bar{P}_{\text{PER}}^{\text{overall}}$. Assume the overall sum of energy consumption in three phases of all devices is limited to E_t, the research problem in this paper is expressed as

$$\underset{\mathcal{C}}{\text{minimize}}\ \bar{P}_{\text{PER}}^{\text{overall}}$$

$$\text{s.t.} \quad \begin{cases} 1 + \mathcal{N}_{\text{CM}} + \mathcal{N}_{\text{Coop}} = \mathcal{N}_{\text{total}} \\ 0 \le \mathcal{N}_{\text{Coop}} \le \mathcal{N}_{\text{total}} - 1 \\ L E_b^{\text{DC}} + E_{\text{AG}} + L_{\text{agg}} E_b^{\text{LB}} + L_c E_b^{\text{LH}} \le E_t. \end{cases} \tag{18}$$

III. Description and Analysis of QPSO Algorithm

PSO is an evolutionary computing technique based on the bird flocking principle. In PSO, a swarm consists of several particles and each particle represents a candidate solution to the optimization problem. In order to find the particle position that can result in the optimum fitness value, each particle flies in the search space and updates its best individual optimum position and global optimum position of the swarm by moving towards a better solution space. QPSO introduces quantum coding mechanism to encode each particle. QPSO tested on some benchmark functions and experimental results showed that QPSO outperforms PSO [23].

A. Qubit-Based Quantum Particle Swarm Optimization

Qubit-based QPSO encodes each particle by a quantum bit (qubit). In [12], a qubit is defined as a pair of composite numbers (ω, β), where $|\omega|^2 + |\beta|^2 = 1$ and $\omega > 0$, $\beta > 0$. $|\omega|^2$ gives the probability that the quantum bit is found in $'0'$ state and $|\beta|^2$ gives the probability that the quantum bit is found in $'1'$ state. Then the quantum velocity of particle m at generation t is

defined as

$$\mathbf{v}_m^t = \begin{bmatrix} \omega_{m1}^t & \omega_{m2}^t & \cdots & \omega_{m\mathcal{R}}^t \\ \beta_{m1}^t & \beta_{m2}^t & \cdots & \beta_{m\mathcal{R}}^t \end{bmatrix} \tag{19}$$

where $m \in [1, 2, \ldots, h]$, h is the number of particles and $\mathcal{R} = \mathcal{N}_{\text{total}} - 1$ that represents the number of cooperative coalition candidates in this paper. Since $\beta_{\text{mn}} = \sqrt{1 - \omega_{\text{mn}}^2}$, we can simplify (19) as

$$\mathbf{v}_m^t = [\, \omega_{m1}^t \ \omega_{m2}^t \ \cdots \ \omega_{mR}^t \,]. \tag{20}$$

The quantum particle position according to (20) can be expressed as

$$x_{\text{mn}}^t = \begin{cases} 1, & \text{if} \quad \delta_{\text{mn}} > (v_{\text{mn}}^t)^2 \\ 0, & \text{if} \quad \delta_{\text{mn}} \leq (v_{\text{mn}}^t)^2 \end{cases} \tag{21}$$

where $\delta_{\text{mn}} \in [0, 1]$ is a uniform random number between 0 and 1. In this paper, the quantum position indicates whether the device n in particle m is a member of the cooperative coalition: $x_{\text{mn}}^t = 1$ represents that the candidate n in particle m is a Coop at generation t; otherwise, the candidate n in particle m is a CM at generation t. Therefore, each particle in this paper represents a possible solution of a particular cooperative coalition, and the fitness value of each particle is obtained by (18).

Denote the fitness value of particle m at generation t to be f_m^t , then the local individual optimum fitness value f_m^{pbest} that is defined as the minimum fitness value of particle m from the first generation to the current generation t and the corresponding local individual optimum position $\mathbf{p}_m$ is defined as follows:

$$f_m^{\text{pbest}} = \min\{f_m^1, f_m^2, \ldots, f_m^t\} \tag{22}$$

$$\mathbf{p}_m = \mathbf{x}_m^{\text{pbest}}. \tag{23}$$

Similarly, the global optimum fitness value f_{gbest} that is defined as the minimum local individual optimum fitness value of all particles and the corresponding global optimum position $\mathbf{p}_g$ is defined as

$$f_{\text{gbest}} = \min\{f_1^{\text{pbest}}, \ldots, f_m^{\text{pbest}}, \ldots, f_h^{\text{pbest}}\} \tag{24}$$

$$\mathbf{p}_g = \mathbf{p}_{\text{gbest}}. \tag{25}$$

At generation $t + 1$, the quantum rotation angle θ_{mn}^{t+1} is updated by

$$\theta_{\text{mn}}^{t+1} = k_1(p_{\text{mn}} - x_{\text{mn}}^t) + k_2(p_{gn} - x_{\text{mn}}^t) \tag{26}$$

where k_1 and k_2 are two positive learning factors of cognitive and social acceleration factors, respectively. The cognitive acceleration factor represents the attraction that a particle has toward its own success and the social acceleration factor represents the attraction that a particle has toward the success of its neighbors. As referred to [24], we set $k_1 = \frac{1}{5}\zeta_1$ and $k_2 = \frac{4}{5}\zeta_2$, where ζ_1 and ζ_2 are Gaussian distributed random numbers with zero mean and unit variance.

The updated velocity of the quantum particle m at $t + 1$ generation is

$$v_{\text{mn}}^{t+1} = \begin{cases} \sqrt{1 - (v_{\text{mn}}^t)^2}, & \text{if } \theta_{\text{mn}}^{t+1} = 0 \text{ and } \delta = c_1 \\ \left| v_{\text{mn}}^t \cos\theta_{\text{mn}}^{t+1} - \sqrt{1 - (v_{\text{mn}}^t)^2} \sin\theta_{\text{mn}}^{t+1} \right|, & \text{otherwise} \end{cases} \tag{27}$$

where δ is a uniform random number between 0 and 1, and c_1 is a constant which refers to the mutation probability, $c_1 \in [0, 1/R]$.

B. Qubit-Based QPSO Cooperative Coalition Selection

The cooperative coalition selection process based on qubit-based QPSO is executed by the capillary gateway. In the network initialization, each device reports its individual information (e.g., residual energy and location) to the capillary gateway. Qubit-based QPSO cooperative coalition selection is summarized in Algorithm 1. Then each device will be informed about their individual role (CH, CM, or Coop) based on the result of Algorithm 1.

Denote the predefined maximum generation to be $T_{\max}$. The research objective of this paper is to minimize the overall PER, that is, the fitness value to guide the particle search is set to be (18). In Algorithm 1, we initialize all quantum particles at first, which is expressed from line 3 to 18. From line 19 to 40, we update the quantum position, velocity, rotation angle, fitness value, local optimum, and global optimum of all particles continuously until reaching the maximum number of generation. Finally, we obtain the global optimum fitness value as the minimized overall PER, as well as the corresponding global optimum position and CH as cooperative coalition from line 41 to line 44.

IV. Simulation Results

A. Performance of QPSO Algorithm

We evaluate the convergence rate and value of qubit-based QPSO algorithm by the Griewank function, which has been employed as a benchmark function for global optimization algorithms.

The Griewank function is defined as follows:

$$F_1(\mathbf{x}) = \frac{1}{4000}\left(\sum_{i=1}^{n}(x_i - 100)^2\right) - \left(\prod_{i=1}^{n}\cos\left(\frac{x_i - 100}{\sqrt{i}}\right)\right) + 1 \tag{28}$$

where $-600 \leq x_i \leq 600$. The global minimum value is 0 and the global minimum is located in the origin, but the function also has a huge number of local minima with regular distribution. Therefore, the difficulty of finding the optimal solution to the Griewank benchmark function is that an optimization algorithm can easily be trapped in a local optimum on its way toward the global optimum.

In the following simulation, we use binary strings to encode the input $\mathbf{x}$ of the Griewank function. For simplification, we set two input variables x_1 and x_2 with the length of 15 bits each. In

Algorithm 1: Qubit-based QPSO for Cooperative Coalition Selection in Order to Minimize the Overall PER.

for each $i \in [1, \mathcal{N}_{\text{total}}]$ **do**
  Set $CH = i$.
  for each $m \in [1, 2, \ldots, h]$ **do**
    for each $n \in [1, 2, \ldots, \mathcal{N}_{\text{total}}]$ **do**
      if $n = CH$ **then**
        Set $x^1_{\text{mn}} = 0$
        Set $v^1_{\text{mn}} = 0$
      else
        Set x^1_{mn} by 0 or 1 randomly
        Set $v^1_{\text{mn}} = 1/\sqrt{2}$
      end if
    end for
    Update f^1_m by (18)
    Set $f^{\text{pbest}}_m = f^1_m$
    Set $\mathbf{p}_m = \mathbf{x}^1_m$
  end for
  Update f_{gbest} by (24)
  Update $\mathbf{p}_g$ by (25)
  for each $t \in [1, 2, \ldots, T_{\max} - 1]$ **do**
    for each $m \in [1, 2, \ldots, h]$ **do**
      for each $n \in [1, 2, \ldots, \mathcal{N}_{\text{total}}]$ **do**
        Update θ^{t+1}_{mn} by (26)
        Update v^{t+1}_{mn} by (27)
        Update x^{t+1}_{mn} by (21)
      end for
      Update f^{t+1}_m by (18)
      if $f^{t+1}_m < f^{\text{pbest}}_m$ **then**
        Set $f^{\text{pbest}}_m = f^{t+1}_m$
        Set $\mathbf{p}_m = \mathbf{x}^{t+1}_m$
      end if
    end for
    Update f^{t+1}_{gbest} by (24)
    if $f^{t+1}_{\text{gbest}} < f_{\text{gbest}}$ **then**
      Set $f_{\text{gbest}} = f^{t+1}_{\text{gbest}}$
      Update $\mathbf{p}_g$ by (25)
    end if
  end for
  Set $f_g(i) = f_{\text{gbest}}$
  Set $\mathbf{p}_g(i) = \mathbf{p}_g$
end for
Set $f_{\text{final}} = \min\{f_g(1), \cdots f_g(i), \cdots f_g(\mathcal{N})\}$
Set the index to obtain f_{final} to be CH_{final}
Set the optimum set of Coops to be $\mathbf{p}_g(CH_{\text{final}})$
return $f_{\text{final}}, CH_{\text{final}}$ and $\mathbf{p}_g(CH_{\text{final}})$

addition, we compare the qubit-based QPSO with three evolutionary algorithms: Ψ-based QPSO, PSO [25], and QGA [26]. We mainly employ the generation updating process of all reference algorithms, and how to formulate them to solve the research problem is similar to qubit-based QPSO. For the four algorithms, we set the population size h to be 20, the dimension of particle R is 30 for two 15 bits input variables. In terms of PSO, the two acceleration coefficients are 2 and velocity limitation is 4. As for QGA, the rotation angle of quantum gates decreases linearly from 0.1π at the first generation to 0.005π at the last generation.

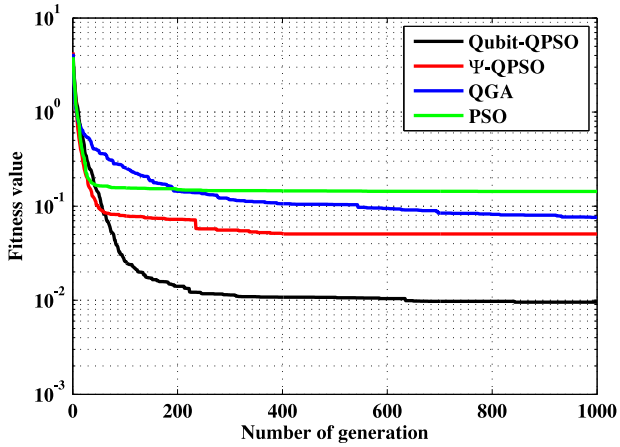

Fig. 2. Number of generations versus fitness value of Griewank function.

TABLE I
SYSTEM PARAMETERS

$M_l = 40$ dB	$N_f = 10$ dB	$N_r = -161$ dBm/Hz
$R_b = 10$ kbps	$G_T\, G_R = 5$ dBi	$\lambda = 0.12$ m
$E_{\text{agg}} = 5$ nJ/bit	$\eta = 0.47$	$L = 1000$ bit
$\mathcal{N}_{\text{total}} = 25$	$\gamma = 0.5$	$P_{\text{LNA}} = 20$ mW
$P_{\text{DAC}} = 15.5$ mW	$P_{\text{mix}} = 30.3$ mW	$P_{\text{filt}} = 2.5$ mW
$P_{\text{filr}} = 2.5$ mW	$P_{\text{IFA}} = 3$ mW	$P_{\text{ADC}} = 9.8$ mW
$F_{\text{block}} = 200$	$\rho_{\text{train}} = 2$	$M = 16$

Fig. 2 shows the convergence value of the four algorithms. It can be seen that the qubit-based QPSO outperforms Ψ-based QPSO, PSO, and QGA algorithms by more accurate convergence value, which is more closer to the global minima 0. Considering the fact that the Griewank function has huge number of local optimum, the result suggests that the qubit-based QPSO has better capacity in getting out of local optimum.

B. Numerical Results of Overall PER Minimization

Assume 25 devices are randomly distributed and located within a square with 100 m side length. The capillary gateway is located at the corner of one side if not otherwise specified in the following simulation. The system parameters are given in Table I. In this scenario, we also simulate PSO [25] and QGA [26] as reference.

First, one of the main difficulties of applying an evolutionary algorithm to a given problem is to decide an appropriate set of parameter values, such as optimum number of particles and optimum number of generations [27]. Denote the optimum number of generations to be T_{opt}, which shows the number of generations required to first produce the final optimum global fitness value. In addition, as referred to [28], the function evaluations denoted by $\mathbb{FE}$ is defined as $\mathbb{FE} = T_{\text{opt}} \times h$, which indicates the algorithm complexity with respect to different number of particles. Table II shows the optimum number of generations and function evaluations for different number of particles to

TABLE II
ALGORITHM COMPLEXITY ANALYSIS OF QUBIT-BASED QPSO

Number of particle (h)	5	10	15	20	25	30	35	40	45	50
Optimum number of generations (T_{opt})	283	117.2	96.85	99.9	83.25	75.1	68.7	71.4	64.15	61.65
Function Evaluations ($\mathbb{FE}$)	1415	1172	1452.75	1998	2081.25	2253	2404.5	2856	2886.75	3082.5

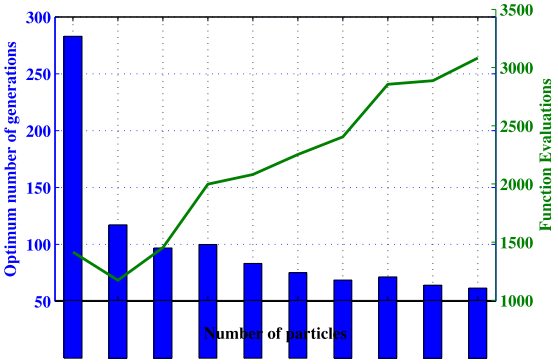

Fig. 3. Convergence time for qubit-based QPSO to converge for different number of particles as measured in optimum number of generations and function evaluations.

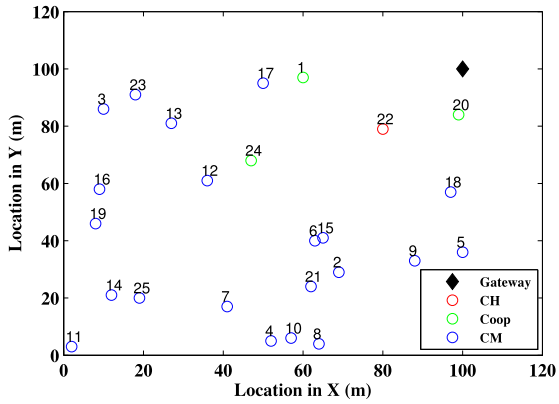

Fig. 4. Device positions and final coalition structure.

converge to the same optimum global fitness value. The simulation iteration is set to be 50 times. In order to emphasize the convergence trend in Table II, Fig. 3 shows the convergence time with respect to both optimum number of generations and function evaluations. It can be seen that a small number of particles may need to run the particle updating process many times and produce lots of particle generations before first producing the global optimum fitness value. On the other hand, Although a large number of particles are able to first reach the global optimum fitness value more quickly, it also means more computation and processing memory contributing to the increase of time complexity. In Fig. 3, the optimum number of generations decreases dramatically from 5 to 20 particles. This is because more particles mean better opportunity to find the optimum fitness value. However, as the number of particles increases from 25 to 50, the optimum number of generations varies within a small range, therefore, the performance of qubit-based QPSO is not sensitive to higher number of particles. Focusing on the function evaluations, it can be seen that the minimum $\mathbb{FE}$ is achieved at the point where the number of particle is 10 and the optimum number of generation is 117.2. Therefore, in order to minimize the algorithm complexity, we set the number of particles to be 10 and number of generations to be 120 (around 117.2) in the following simulation.

Fig. 4 illustrates the position of all devices and the final cooperative coalition structure by the proposed qubit-based QPSO algorithm. The capillary gateway is located at (100 m,100 m). We set the energy constraint E_t to be 0.4 J. The final cooperative coalition consists of device 22, device 1, device 20, and device 24, where device 22 is the CH and the rest are Coops. In general, devices close to the gateway is more likely to be selected as cooperative coalition.

Next, we make a comparison of overall PER in (17) between the four evolutionary algorithms in Fig. 5. Obviously, the

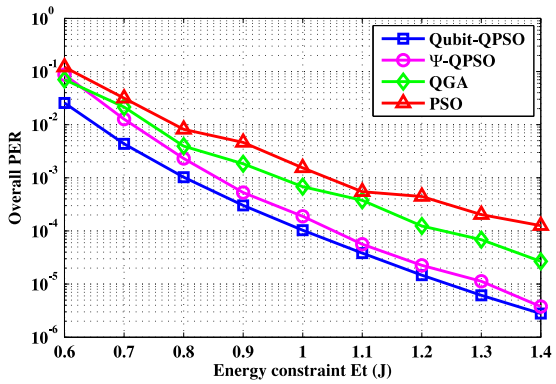

Fig. 5. Energy constraint E_t versus overall PER.

qubit-based QPSO outperforms other three algorithm under the same energy constraint. Moreover, we can see that the overall PER is lower than 10^{-5} for qubit-based QPSO after 1.2 J, therefore if we have to ensure successful transmission from all devices to the capillary gateway, the whole network ought to supply at least 1.2 J and select optimum cooperative coalition by qubit-based QPSO.

In addition, we compare the number of selected Coops of all evolutionary algorithms in terms of energy constraint in Fig. 6. The scenario setting is the same with Fig. 5. It can be seen that the number of Coops selected by the qubit-based QPSO is not always the highest. Considering the result that the overall PER of qubit-based QPSO outperforms the other three algorithms in terms of energy constraint, as indicated in Fig. 5, we can conclude that higher number of Coops is not necessary and qubit-based QPSO can select different number of optimum Coops dynamically according to different scenario setting. In addition, as for qubit-based QPSO algorithm, the selected number of coops increases slowly with respect to the energy

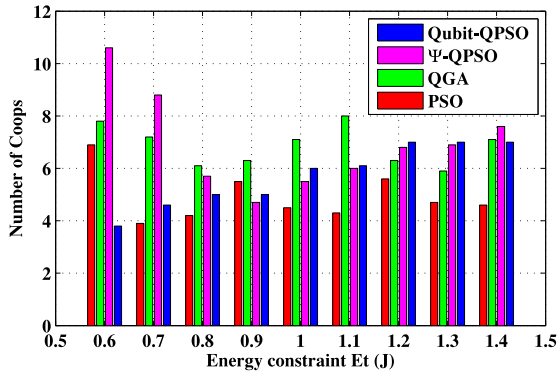

Fig. 6. Energy constraint E_t versus number of Coops.

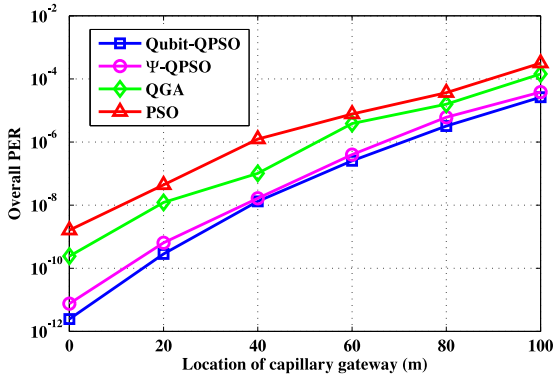

Fig. 7. Location of capillary gateway versus overall PER.

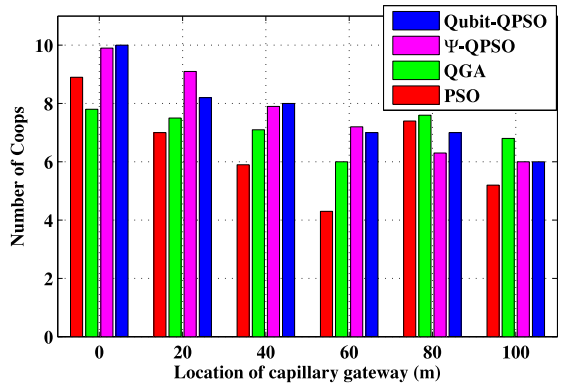

Fig. 8. Location of capillary gateway versus number of Coops.

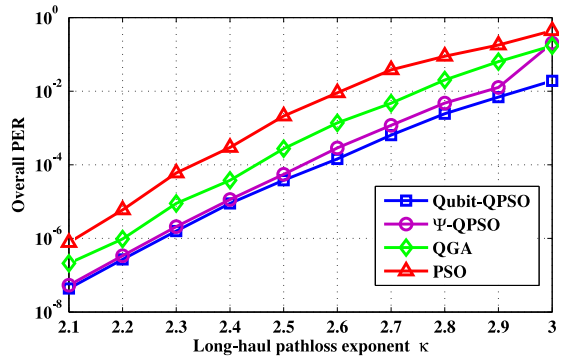

Fig. 9. Long-haul channel condition versus overall PER.

constraint. Particularly, the number of Coops remains to be 7 at 1.2, 1.3, and 1.4 J, because the additional suitable Coops cannot be found.

Fig. 7 takes the location of capillary gateway into consideration. We set E_b to be 0.8 J. The x-axis in Fig. 7 is the relative location from the capillary gateway to the edge corner of the predefined scenario, e.g., $x = 20$ indicates that the gateway is located at (120 m,120 m) if the edge of scenario is (100 m,100 m). It is observed that the two QPSO algorithms outperform PSO and QGA significantly. Moreover, the location of capillary gateway is closely related to the LH distance, which indicates that the PER of LH transmission dominates the overall PER in the farther LH distance. Thus, more energy supply is expected to guarantee successful transmission in the scenario of farther capillary gateway.

Fig. 8 investigates the number of Coops with respect to different location of capillary gateway. The scenario setting is the same with Fig. 7. In general, more Coops can be selected in order to decrease the overall PER under the same energy constraint. As for QPSO algorithm, the number of optimum Coops decreases with the increase of the relative distance from the scenario to the capillary gateway, which is caused by the higher energy consumption of the LH transmission phase.

Finally, Fig. 9 depicts the overall PER in terms of LH path loss exponent. We set E_b to be 1.2 J. We see that the overall PER performs worse with the increase of LH path loss exponent κ, because the PER in LH transmission becomes dominant. Additionally, qubit-based QPSO outperforms other three algorithms.

V. Conclusion

In this paper, we investigate the CH and Coops cooperative coalition selection using qubit-based QPSO algorithm with the aim of minimizing the overall PER in cluster-based capillary networks. We show that CH and Coops can effectively form a cooperative MISO system in the LH transmission. Additionally, qubit-based QPSO algorithm is applied in order to select best coalition of Coops for the potential CH. Compared with other evolutionary algorithm, we proved that qubit-based QPSO has advantages of better evolutionary equations, simpler updating equations, and faster convergence speed. Finally, simulation results show that the proposed qubit-based QPSO scheme outperforms Ψ-based QPSO, PSO, and QGA in terms of overall PER.

References

[1] Y. Li, K. K. Chai, Y. Chen, and J. Loo, "Duty cycle control with joint optimisation of delay and energy efficiency for capillary machine-to-machine networks in 5g communication system," *Trans. Emerg. Telecommun. Technol.*, vol. 26, pp. 56–69, 2015.

[2] V. Misic, J. Misic, and D. Nerandzic, "Extending LTE to support machine-type communications," in *Proc. IEEE Int. Conf. Commun.*, Jun. 2012, pp. 6977–6981.

[3] A. Coso, S. Savazzi, U. Spagnolini, and C. Ibars, "Virtual MIMO channels in cooperative multi-hop wireless sensor networks," in *Proc. 40th Annu. Conf. Inf. Sci. Syst.*, 2006, pp. 75–80.

[4] H. Xiao and S. Ouyang, "Power control game in multisource multirelay cooperative communication systems with a quality-of-service constraint," *IEEE Trans. Intell. Transp. Syst.*, vol. 16, no. 1, pp. 41–50, Feb. 2015.

[5] Y. Chen, C. X. Wang, H. Xiao, and D. Yuan, "Novel partial selection schemes for AF relaying in nakagami- m fading channels," *IEEE Trans. Veh. Technol.*, vol. 60, no. 7, pp. 3497–3503, Sep. 2011.

[6] A. Del Coso, U. Spagnolini, and C. Ibars, "Cooperative distributed MIMO channels in wireless sensor networks," *IEEE J. Sel. Areas Commun.*, vol. 25, no. 2, pp. 402–414, Feb. 2007.

[7] S. Cui, A. Goldsmith, and A. Bahai, "Energy-efficiency of MIMO and cooperative MIMO techniques in sensor networks," *IEEE J. Sel. Areas Commun.*, vol. 22, no. 6, pp. 1089–1098, Sep. 2004.

[8] Y. Yuan, Z. He, and M. Chen, "Virtual MIMO-based cross-layer design for wireless sensor networks," *IEEE Trans. Veh. Technol.*, vol. 55, no. 3, pp. 856–864, May 2006.

[9] L. Bai, L. Zhao, and Z. Liao, "Energy balance in cooperative wireless sensor network," in *Proc. 14th Wireless Conf.*, Jun. 2008, pp. 1–5.

[10] D. Wu, Y. Cai, L. Zhou, and J. Wang, "A cooperative communication scheme based on coalition formation game in clustered wireless sensor networks," *IEEE Trans. Wireless Commun.*, vol. 11, no. 3, pp. 1190–1200, Mar. 2012.

[11] L. Song, K. K. Chai, Y. Chen, J. Schormans, J. Loo, and A. Vinel, "QoS-aware energy efficient cooperative scheme for cluster-based IoT systems," *IEEE Syst. J.*, 2016.

[12] H.-Y. Gao, J.-L. Cao, and M. Diao, "A simple quantum-inspired particle swarm optimization and its application," *Inf. Technol. J.*, vol. 10, no. 12, pp. 2315–2321, 2011.

[13] J. Sun, B. Feng, and W. Xu, "Particle swarm optimization with particles having quantum behavior," in *Proc. Congr. Evol. Comput.*, 2004, vol. 1, pp. 325–331.

[14] J. Cao, T. Zhang, Z. Zeng, Y. Chen, and K. K. Chai, "Multi-relay selection schemes based on evolutionary algorithm in cooperative relay networks," *Int. J. Commun. Syst.*, vol. 27, no. 4, pp. 571–591, 2014.

[15] T. H. Lee, *The Design of CMOS Radio-Frequency Integrated Circuits*. Cambridge, U.K.: Cambridge Univ. Press, 2004.

[16] Y. Gai, Y. Zhang, and X. Shan, "Energy efficiency of cooperative MIMO with data aggregation in wireless sensor networks," in *Proc. Wireless Commun. Netw. Conf.*, Mar. 2007, pp. 791–796.

[17] A. Wang, W. Heinzelman, and A. Chandrakasan, "Energy-scalable protocols for battery-operated microsensor networks," in *Proc. IEEE Workshop Signal Process. Syst.*, 1999, pp. 483–492.

[18] Y. Yuan, M. Chen, and T. Kwon, "A novel cluster-based cooperative MIMO scheme for multi-hop wireless sensor networks," *EURASIP J. Wirel. Commun. Netw.*, vol. 2006, no. 2, pp. 38–38, Apr. 2006. [Online]. Available: http://dx.doi.org/10.1155/WCN/2006/72493

[19] S. K. Jayaweera, "Energy analysis of MIMO techniques in wireless sensor networks," in *Proc. 38th Conf. Inf. Sci. Syst.*, 2004.

[20] L. Dai and Q. Zhou, "Energy efficiency of MIMO transmission strategies in wireless sensor networks," in *Proc. Int. Conf. Comput. Commun. Control Technol.*, 2004, vol. 1, Art. no. 2.

[21] Y. Zhang and H. Dai, "Energy-efficiency and transmission strategy selection in cooperative wireless sensor networks," *J. Commun. Netw.*, vol. 9, no. 4, pp. 473–481, Dec. 2007.

[22] R. Khalili and K. Salamatian, "A new analytic approach to evaluation of packet error rate in wireless networks," in *Proc. 3rd Annu. Commun. Netw. Services Res. Conf.*, May 2005, pp. 333–338.

[23] S. Mikki and A. Kishk, "Quantum particle swarm optimization for electromagnetics," *IEEE Trans. Antennas Propag.*, vol. 54, no. 10, pp. 2764–2775, Oct. 2006.

[24] J. Cao, T. Zhang, Z. Zeng, and D. Liu, "Interference-aware multi-user relay selection scheme in cooperative relay networks," in *Proc. Globecom Workshops*, Dec. 2013, pp. 368–373.

[25] N. Latiff, C. Tsimenidis, and B. Sharif, "Energy-aware clustering for wireless sensor networks using particle swarm optimization," in *Proc. IEEE 18th Int. Symp. Personal, Indoor Mobile Radio Commun.*, 2007, pp. 1–5.

[26] J. Yang, B. Li, and Z. Zhuang, "Research of quantum genetic algorith and its application in blind source separation," *J. Electron.*, vol. 20, no. 1, pp. 62–68, 2003.

[27] F. Lobo, C. Lima, and Z. Michalewicz, *Parameter Setting in Evolutionary Algorithms*, 1st ed. New York, NY, USA: Springer, 2007.

[28] S. Chen, J. Montgomery, and A. Bolufé-Röhler, "Measuring the curse of dimensionality and its effects on particle swarm optimization and differential evolution," *Appl. Intell.*, vol. 42, no. 3, pp. 514–526, 2014. [Online]. Available: http://dx.doi.org/10.1007/s10489-014-0613-2

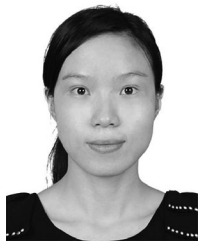

Liumeng Song (GS'14–M'16) received the B.E. degree from the Beijing University of Posts and Telecommunications, Beijing, China, in 2012. She is currently working toward the doctoral degree at the School of Electronic Engineering and Computer Science, Queen Mary University of London, London, U.K.

Her research interests include machine learning, energy efficiency, clustering and cooperative communication.

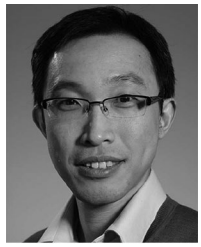

Kok Keong Chai received the B.Eng. (Hons.), M.Sc., and Ph.D. degrees in 1998, 1999, and 2007, respectively.

He is an Internet of Things Programme Leader and a Lecturer of the Joint Programme between Queen Mary University of London (QMUL), London, U.K., and the Beijing University of Posts and Telecommunications, Beijing, China. He is a Senior Lecturer of the Networks Research Group, QMUL. His current research interests include cooperative multiple-input–single-output transmission scheme, dynamic resource management wireless communications, medium access control for machine to machine communications and networks, and sensing and prediction in distributed smart grid networks.

Yue Chen (S'02–M'03–SM'15) received the B.Eng., M.Eng., Ph.D., MIET, and MIEEE degrees.

She joined the Networks Research Group, Queen Mary University of London (QMUL), in 2000 and continued as a Member of Staff in 2003 after receiving the Ph.D. degree in wireless communications. She is currently a Professor and the QMUL Director of the Joint Programme with the Beijing University of Posts and Telecommunications (BUPT), Beijing, China. She has been involved in numerous research activities and her research interests focus on intelligent radio resource management for wireless networks, cognitive and cooperative wireless networking, HetNet, Smart energy systems, and Internet of Things.

Jonathan Loo (M'01) received the M.Sc. degree in electronics (with distinction) and Ph.D. degree in electronics and communications from the University of Hertfordshire, Hertfordshire, U.K., in 1998 and 2003, respectively.

From 2003 to 2010, he was a Lecturer in multimedia communications with the School of Engineering and Design, Brunel University, Uxbridge, U.K. Since 2010, he has been an Associate Professor of communication networks with the School of Science and Technology, Middlesex University, London, U.K. He leads a research team in the area of communication and networking. His research interests include wireless communication, network architecture, communication protocols, wireless and mobile networks, network security, embedded systems, video coding and transmission, digital signal processing, and optical networks. He has successfully graduated 14 Ph.D. students. He has coauthored more than 175 journal and conference papers in the aforementioned specialist areas. He was the Lead Editor of *Mobile Ad Hoc Networks: Current Status and Future Trends* (CRC Press, 2011).

Dr. Loo has been an Associate Editor of Wiley's *International Journal of Communication Systems* since 2011.

John Schormans received the B.Sc. (Eng.), Ph.D., C.Eng., MIET, and FHEA degrees.

He joined Queen Mary University of London (QMUL), London, U.K. as a Lecturer in 1994. He is currently a Senior Lecturer with the Networks Research Group, QMUL. His research interests include the application of probabilistic methods to the analysis, simulation, and performance measurement of packet-based communications systems and networks. In these research areas he has been a Principal Investigator for the U.K.'s Engineering and Physical Sciences Research Council. He has authored or coauthored more than 140 papers and 2 books.